

*Elbakari, Ramy, and Medhat H. Shehata. "A Proposed Laboratory Method to Evaluate the Durability of Concrete Pavement Joints Against Freezing in the Presence of Deicer Salts." Canadian Journal of Civil Engineering, 02/2022,*

*doi:10.1139/cjce-2021-0140.*

# **A Proposed Laboratory Method to Evaluate Durability of Concrete Pavement Joints against Freezing in the Presence of Deicer Salts**

**Ramy Elbakari and Medhat H. Shehata\***

Department of Civil Engineering, Ryerson University

\*: corresponding author: [mshehata@ryerson.ca](mailto:mshehata@ryerson.ca)

## **Abstract**

Deicer salts were found to cause deterioration to the concrete pavement, particularly at joints. This paper introduces a laboratory procedure that engineers and scientists can use to evaluate the durability of joints. Concrete samples were tested under different salt concentrations and exposure conditions, including freeze-thaw cycles, wet-dry cycles, and a combination thereof. The test sample comprises a square slab measuring 200x200x120 mm and a joint running in the middle at 40 mm depth. The results showed that the test method needs to include two salts with two exposure conditions for accelerated damage. The first exposure uses NaCl at 10% concentration with 50 cycles of freeze/thaw-wet/dry alternating every five consecutive cycles. The second exposure uses CaCl<sub>2</sub> at 15% concentration with 50 cycles of wetting and drying at 5°C and 35 °C, respectively. Damage is assessed using two approaches: 1) strength loss under flexural loading and 2) visual damage.

## **Keywords**

Concrete pavements, joint deterioration, freezing and thawing, deicing salts, wetting and drying, test methods.

## **1. Introduction**

Concrete joints are defined by their primary function. The most common type of transverse joints in concrete pavements are contraction joints which allow concrete to shrink or contract without forming random cracks in locations other than the joints. There are different types of contraction joints that are classified based on the shape, method of forming, and geometry (Delatte 2014; Mallick and El-Korchi 2013; Federal Highway Administration 2019). Control joints are a form of contraction joints that provide a weakened vertical plane to define the location of cracking. Control joints are pre-molded in the fresh concrete or formed, more commonly, via saw cutting the placed concrete at regular intervals. The time window for saw cutting is very critical. The concrete must have enough strength to allow sawing without causing damage and raveling around the joint. Also, the sawing must not be delayed that the concrete would crack before creating the joint. There are different saw sizes and shapes that can be designed in a control joint (Federal Highway Administration 2019, Chan et al. 2020). Some joints can be of fixed width throughout their depth, while others can have a wider reservoir in their top half to accommodate a backer rod and sealant (Chan et al. 2020). The depth of joint should be enough to create a weak section without going through the load transfer device or the dowels commonly used in transverse joints of concrete pavements or tie bars in case of longitudinal joints (Federal Highway Administration 2019).

During winter, deicer salts are used on concrete pavements to depress water's freezing temperature and deter ice formation on roads (Chan et al. 2020). Three common salts are used: sodium chloride, calcium chloride, and magnesium chloride (Ghazi et al. 2018, OPSS 2021). Eventually, the deicer salts get absorbed into the concrete pavement and can cause severe damage (Ghazi et al. 2018, Xie et al. 2020, Wang et al. 2018). The damage is much observed in

the vicinity of control joints - as salt solution accumulates inside the joints (Taylor et al. 2016, Chan et al. 2020, Ghazi et al. 2018, Wang et al. 2018) - and is believed to be caused by one or a combination of the following: 1) concrete exposure to cycles of freezing and thawing in a saturated condition (Jones et al. 2013), and 2) exertion of internal stresses in the pores of the concrete as a result of crystallization of the salts (Ghazi et al. 2018, Ghazi and Bassuoni 2019) or products formed from chemical interactions between cement paste and deicer salts (Jones et al. 2013, Thaulow et al. 2004, Taylor et al. 2016, Wang et al. 2018, Ghazi and Bassuoni 2019). The crystallization products can form in the entrained air voids; in such cases, the air voids become occupied by the products and lose the capacity to accommodate the increase in the volume of water in concrete upon freezing. Hence, the crystallization of salt or the formation of reaction products between the deicers and cementing materials in air voids reduces the resistance of the concrete to cycles of freezing and thawing (Jones et al. 2013, Thaulow et al. 2004, Taylor et al. 2016, Ghazi et al. 2018).

It has been reported that saw-cut joints are more prone to damage than formed joints (Zhang et al. 2015, Wang et al. 2018) – likely due to solution penetrating the concrete through the interfacial transition zone (ITZ) of the aggregate exposed through the saw cutting process. Enhancing ITZ was found to increase the resistance to the damage observed in joints (Zhang et al. 2015)

When applied as a deicer salt in the winter season, calcium chloride can be absorbed into the concrete and alter the microstructure of the concrete, causing damage (Farnam et al. 2015a, Ghazi et al. 2018). The damage can occur in the winter or later without freezing temperature if enough

amount is absorbed in concrete. The damage can be severe cracking and deterioration due to the formation of calcium oxychloride (Farnam et al. 2015a, Taylor et al. 2016, Jones et al. 2020). This compound - calcium oxychloride - results from a chemical reaction between calcium chloride and calcium hydroxide, which is abundantly available in hydrated cement systems (Farnam et al. 2015a, Jones et al. 2020). In addition, calcium chloride can also form other compounds such as Friedel's salt and Kuzel's salt (Farnam et al. 2015a, Ghazi and Bassuoni 2019). The formation of calcium oxychloride proceeds above the freezing point of water (Farnam et al. 2015a). However, as the salt concentration increases, calcium oxychloride forms from unfrozen solution at lower temperatures (Qiao et al. 2018c, Wang et al. 2019). Calcium oxychloride formation is expansive and produces internal pressure in the concrete matrix, causing cracks (Chatterji et al. 1978, Taylor et al. 2012, Jones et al. 2020).

When sodium chloride is applied as a deicer salt to pavements, some get absorbed by the concrete (Ghazi et al. 2018), and the chloride can get adsorbed onto the surface of calcium-silicate hydrate (C-S-H) (Qiao et al. 2018b). Chloride ions can also react chemically with the cement paste, specifically with the aluminate and aluminoferrite phases, forming Friedel's salt and Kuzel's salt (Qiao et al. 2018b). Some researchers believe that the crystallization of Friedel's salt exerts pressure against the pore walls of the cement paste, which leads to damage and strength reduction (Qiao et al. 2018b).

Magnesium chloride is the most effective deicer salt in depressing freezing temperatures. When used at relatively lower concentrations, it lowers the freezing temperature more than any other deicer salt (Farnam et al. 2018c). It is considered the most deteriorating deicer salt due to its reaction with a wide range of cement paste constituents including, calcium hydroxide, calcium silicate hydrate, and aluminate phases (Farnam et al. 2018c, Ghazi and Bassuoni 2019, Xie et al.

2019). This reaction leads to the formation of brucite, magnesium calcium hydrate, calcium oxychloride, and magnesium oxychloride. All the formed compounds weaken the concrete due to their unbinding nature and depletion of the cement paste matrix (Farnam et al. 2018c). Besides, the expansive products formed increase the internal pressure, leading to deterioration similar to sodium chloride and calcium chloride deteriorations discussed previously.

Magnesium chloride primary reacts with the two main constituents of cement paste  $\text{Ca(OH)}_2$  and C-S-H forming brucite and M-S-H, respectively. When the brucite formation occurs near the concrete's surface, the precipitation of the brucite forms an outer layer that hinders the ingress of more deicer salts (Farnam et al. 2018c).

This paper introduces a laboratory method to evaluate the durability of control joints in concrete pavements under conditions that represent the environment in Canada. Currently, there are no standard test methods for the evaluation of joint durability. There are, however, test methods that evaluate freezing and thawing of concrete (ASTM C 666) and salt scaling (CSA A23.2-22C) due to ponding of deicer salts. Nevertheless, both tests do not address the unique damage mechanism that takes place within joints. The ASTM C666 evaluates the concrete resistance to freezing/thawing in the absence of deicer salts, while CSA A23.2-22C evaluates the damage on the surface of concrete due to freezing/thawing cycles in the presence of salts. None of the two standard test methods evaluates damages in joints or the deterioration that might occur over the service life of concrete due to wetting/drying in warm seasons after the concrete absorbs the deicers applied during the winter seasons. The ASTM C 666 has been used with some modifications (Ghazi and Bassuoni 2019) to evaluate different cementing blends under freezing and thawing and wetting/drying cycles in the presence of salts. In addition, concrete cylindrical samples were also

tested (Xei et al. 2019) to evaluate materials under different cycles. However, the reported investigation did not enable evaluating different joint dimensions, design, or the effect of construction practice, such as curing and forming the joints, on their durability or long-term serviceability – this is the intention of this paper.

## **2. Research Significance**

Since deterioration in concrete pavement joints occurs at an early stage of pavement service life (Chan et al. 2020), it is of interest to develop or put the basis for a test method to assess the durability of control joints. This paper examines different exposures and salt types/concentrations to establish the test conditions, including salt types, that lead to obtaining the results in a relatively short time. The test is intended to be used to evaluate or compare the durability of different designs of control joints, including joint width and shape and method of joint fabrication (pre-moulded or saw cutting). The novelty of this study lies in (i) it is a new test method that evaluates the joint as constructed in the actual pavement. There is no current standard test to evaluate the durability of joints, (ii) The test is designed to capture construction method (e.g., saw cutting) and seasonal variation, including freezing/thawing and wetting/drying that takes place over the four seasons. Testing cycles of freezing/thawing without wetting/drying may not reflect the damage that concrete experiences in the summer during wetting (rain) and drying (high temperature); (iii) The test can also be used to evaluate concrete strength, concrete composition, curing method, or different salt type and concentrations on the damage. The fact that the test is applied to an actual joint strengthens the relevance of the obtained results.



### **3. Experimental Program**

#### **3.1. Mixture proportioning**

The concrete used here had a w/c of 0.56 without Supplementary Cementing Materials (SCM). While this mixture is of lower quality than a typical pavement mix, it was used here to accelerate the deterioration to establish the conditions - salt type/concentrations and types of cycles - that cause the most noticeable or measured damage. This w/c produced a 28-day compressive strength of 25 MPa ( $\pm 1$  MPa). This mix is referred to here as 25 MPa mix.

The coarse limestone aggregate was obtained from Niagara escarpment and had a dry-rodded density of 1686.2 kg/m<sup>3</sup>. The fine aggregate was obtained from Caledon, Ontario. No water reducer was needed because the workability was acceptable at the given w/c ratio. An air-entraining admixture conforming to ASTM C 260 was used, and an air content between 4-6% was obtained across all slabs. It should be noted that the requirement for pavement concrete in Canada is to have an entrained air of 5 - 8%. The impact of allowing less air content here would be a faster deterioration. The mix proportion used in the slabs was as follows:

Cement	270 kg
Coarse Aggregate	1079 kg
Fine Aggregate	790 kg
Water	151.2 kg
Air Entrainer	204 mL

#### **3.2. Test Samples**

The geometry of the specimen was selected to mimic control joints. The test specimen was a square slab of dimensions 200 mm x 200 mm x 120 mm with a control joint runs in the middle of the slab at one-third of the depth, measuring 40 mm. The joints' depth and the slab dimensions were chosen to allow for sufficient joint exposure to deicer salts while keeping the sample size adequate for

casting and handling. The samples (slabs) have dimensions different from the slabs used in the salt scaling test (CSA A23.2-22C) - particularly the thickness - as the intention here is to test the joint rather than the surface in the case of CSA A23.2-22. In the current test, the solution is introduced inside the joint instead of on the surface of the slab, as in the case of CSA A23.2-22.

### **3.3. Sample preparation and conditioning**

Each sample tested under a specific exposure condition consisted of three slabs (specimens). Slabs were cast twenty at a time to limit variability between the samples. Six sets of three slabs for a total of eighteen slabs were used from each cast. The slabs were cast in two moulds holding ten slabs each, as shown in Fig. 1. A poker vibrator was used to consolidate the concrete and was run through each slab individually. After the slabs were cast and consolidated, they were covered by wet burlap and a tarp sheet to allow for curing. They remained covered by the tarp for 16 hours before cutting the joint. The saw cutting operation took place by fixing two steel railing over the moulds and running a saw blade through the concrete. This ensured that all ten slabs had the same cut depth of around 40 mm. The saw cutting was done to mimic construction practice and produce the microcracking that might be developed as a result of this process under field conditions. The slabs were then moved to a standard shrinkage room of 50% relative humidity (RH) and room temperature ( $21 \pm 2$  °C) for eleven days, where they were allowed to dry. The short wet curing period (16 hours) represents a case of very ineffective curing on-site. The drying period in the shrinkage room was adopted to allow the salt solution - to be applied during the testing - to penetrate the concrete faster.

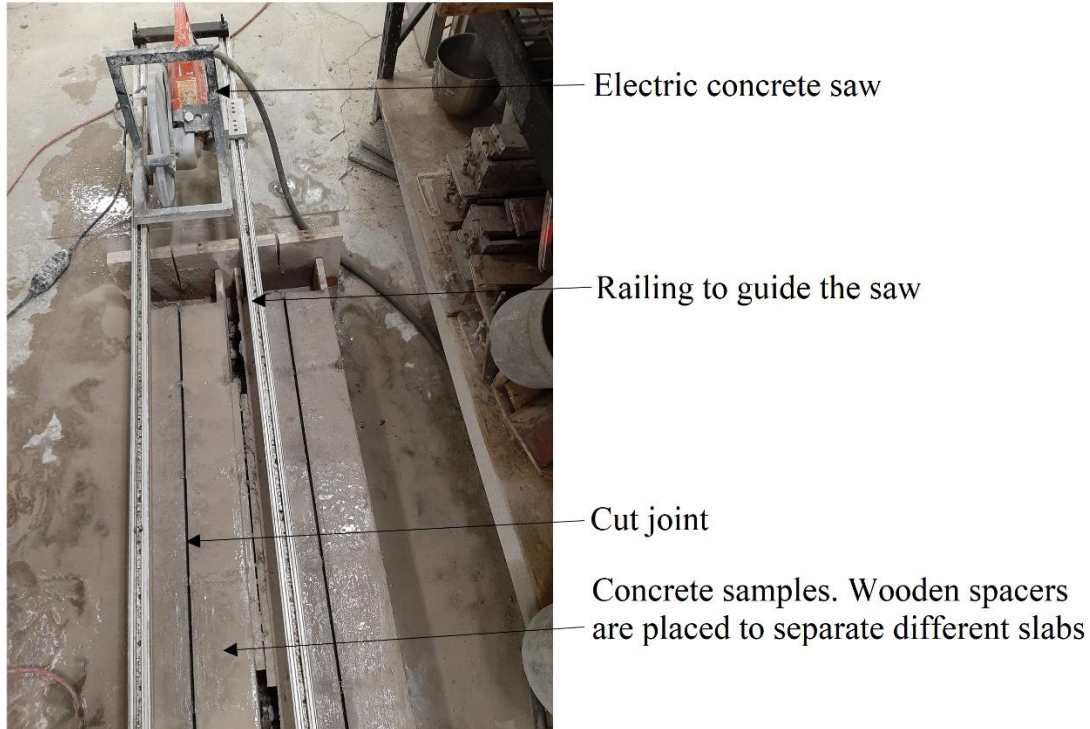


**Fig. 1.** Moulds with railing to enable accurate saw cutting of the joints after hardening

The slabs remained for eleven days in the shrinkage room before having both ends of the saw cut enclosed to hold a solution within the joint (Fig. 2). Enclosure took two days for the silicone-based adhesive to dry on both sides of the joint. As such, the slabs started their exposure cycles after 14 days from the day of casting. Enclosing both ends of the saw cut is required to contain the salt solution inside the joint. Fig 2 displays a slab after having both ends enclosed.

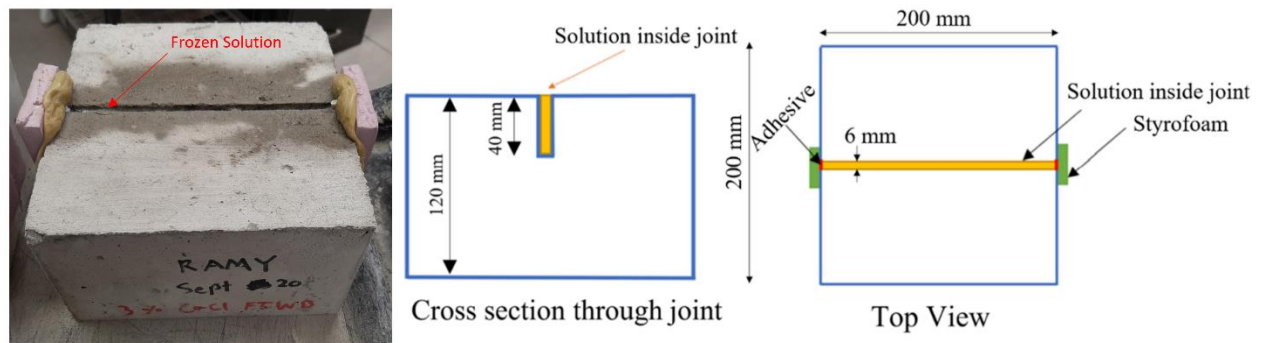


**Fig 2.** A schematic of a test slab after being enclosed on both ends of the joint and filled with the solution

### **3.4. Exposure Conditions**

The exposure conditions are designed to capture the freezing and thawing and its associated pressure and the chemical reactions when the salts ingress through the concrete. Three exposure conditions were used here: freeze-thaw cycles, wet-dry cycles, and a combination thereof. Various salt concentrations are used, including 10%, and 15% (wt. %) of different salts. The following paragraphs describe the exposure conditions:

#### **1. Freeze-Thaw (FT) Cycles**

The freeze-thaw cycles are composed of freezing a salt solution in the joint at -18 °C for 16 hours, followed by a thaw cycle at room temperature for 8 hours. If the salt solution level dropped due to evaporation, absorption, and minor leakage, the joint would get refilled with the solution to the top during the following cycle. A total of 50 freeze-thaw cycles are adopted, and thus, it takes 50 days to complete this test.

#### **2. Wet-Dry (WD) Cycles**

The wet-dry cycles involve filling the joint with a salt solution, which finds its way to the concrete in the joints' vicinity through diffusion and wicking. According to Qiao et al. (2018c), it was shown that the formation of calcium oxychloride is more sustained at 5°C, and therefore the wetting part of the cycle took place at this temperature. The wetting duration was set to 24 hours to allow for sufficient time for the solution to penetrate the concrete and react with its constituents. This wetting cycle was followed by another 24 hours of drying at 35°C in a drying oven. The drying cycle represents the low humidity and warm temperature the pavement experiences during its service life. The drying allows for the salt crystallization and its associated pressure to put stresses on the concrete. The WD exposure is composed of 50 cycles, but - unlike the freezing/thawing exposure - it would span 100 days instead of 50 days due to its longer cycles. The timing for the WD cycles

was chosen to ensure sufficient wetting of the slabs followed by complete drying at the bottom of the joint. This took longer than FT cycles since the latter only required freezing and thawing of ice.

### 3. Freeze-Thaw-Wet-Dry (FTWD) Cycles

A combination of both freeze-thaw and wet-dry cycles forms the third exposure type. The samples were made to alternate after five consecutive cycles of each exposure. The first five cycles were freezing and thawing, leaving the last five to be wetting and drying. This third exposure would require 25 days for the freezing and thawing component and 50 days for wetting and drying, adding up to 75 days in total.

### 4. Control Cycles

Control samples were tested under the same exposure but without salts to determine the comparative effect of each exposure condition. Since all exposure conditions apply moisture (solution) to the samples, the concrete would experience further hydration during the process. Thus, the control samples were tested in FT, WD, and FTWD cycles with only water in the joint. In other words, the control samples were put to experience similar hydration as the remaining samples, but not the deterioration associated with the use of salt. Table 1 provides a summary of the test methods included in this study.

Table 1: Test matrix and labels of cycles.

<b>Exposure Condition/De-icer Salt</b>	<b>Freeze-Thaw (FT)</b>	<b>Wet-Dry (WD)</b>	<b>Freeze-Thaw-Wet-Dry (FTWD)</b>
<b>Cycle Type/ and duration</b>	16-hour freezing 8-hour thawing	24-hour wetting 24-hour drying	16-hour freezing 8-hour thawing  24-hour wetting 24-hour drying
<b>Salt Concentrations*</b>	10%	10% & 15%	10%
Total number of cycles	50	50	50
Total Duration	50 days	100 days	75 days
*Three salts were used in each case, CaCl <sub>2</sub> , NaCl, and MgCl <sub>2</sub>			

### 3.5. Methods of Assessments

This study adopted two assessment methods: (i) visual inspection and (ii) slab strength under bending.

#### i) Visual Damage Assessment

In this method, the slabs were inspected for visible damages, including cracking and spalling. Besides, the joints were broken-open to examine the inner sides of the joints for deterioration. To break-open the slab joints, the slabs were inverted and loaded in bending on the mid-point. The joint acted as a notch, which made it easy to break the slab at that location and expose the sides of the joints. The load and deformation captured during loading were used as the second assessment method, as explained in this coming paragraph.

#### ii) Bending Test of the Slabs

The damage inflicted on the concrete can be manifested through the weakening of the concrete thickness underneath the joint. Some chemical reactions with deicer salts are expected to affect

concrete mechanical properties (Heukamp et al. 2001, Xie et al. 2019, Wang et al. 2019). Hence, the slabs were subjected to flexural failure through a three-point loading as another way - besides visual evaluation - to detect deterioration in the samples, as shown in Fig. 3. The loading does not necessarily represent the field condition, but it serves to detect deterioration. The test was similar to the standard third point test, except the sample used here is a slab with a joint rather than a beam. In total, there were three slabs for each exposure condition. However, due to the size of the slab and - in some cases - inadequate compaction near the ends of the slabs, a limited number of specimens failed in shear and were eliminated from the results. Force at failure and horizontal tensile stresses at the base or bottom of the joint were determined and used to compare the effects of various exposure conditions.

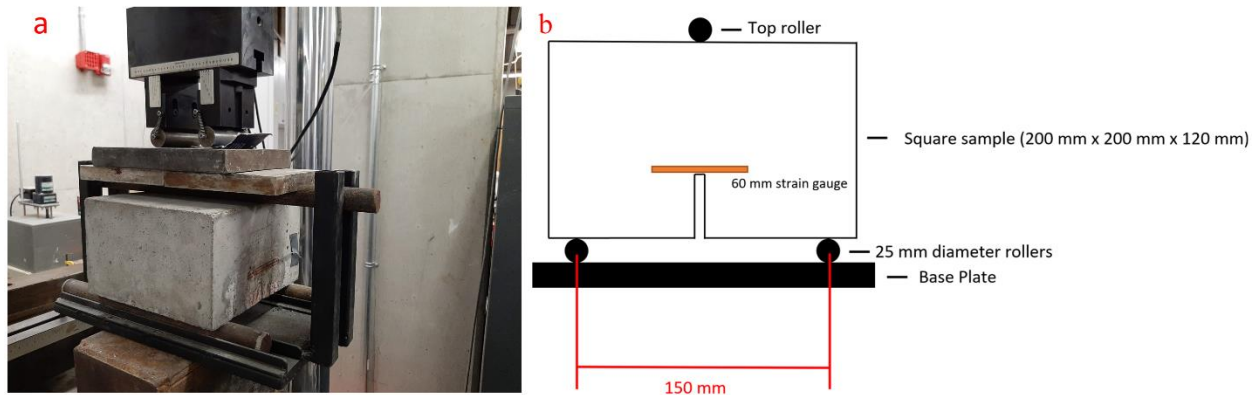


**Fig.3.** a) Three-point loading of slabs b) Slab dimensions and loading condition

During loading, the force loading history produced by the hydraulic machine was recorded until failure. Two strain gauges were attached at each end of the slab at the bottom of the joint to measure strain values during loading. By knowing the force applied and the strain produced, a non-linear finite element analysis was conducted to determine the stresses produced at each time step. Ideally, the force and concrete modulus of elasticity are required to determine the strain and stress in an

element (Bathe 2005). Since the concrete deteriorates during the exposure, its modulus of elasticity at the time of testing is unknown. Through an iterative approach, the modulus of elasticity was determined to be the value that produced the measured strain. The stress could then be determined from the deduced material modulus, and - finally - the stress-strain curve at the location just at the bottom of the joint can be graphed. The use of stress values produced by the finite element model is believed to produce more accurate results than the force at failure - as the effects of geometric imperfections and crack propagation during failure are minimized compared to force values. Deviations in joint width and location might skew force values; also, shear crack formation might go unnoticed without stress-strain curves. For this reason, both force and stress-strain curves were investigated. However, in the current study, considering the stress-strain curves or force at failure did not change the outcomes or the results or the conclusions, as will be shown.

Finally, due to strain measurement limitations, only data until 100  $\mu$ -strain were used. The strain gauges continued to read the strain until they experienced breakage, which does not coincide with concrete cracking or failure. Accordingly, strain measurements after 100  $\mu$ -strain are not reliable. When reporting the maximum stress used herein the analysis, the stress value at 100  $\mu$ -strain was taken unless the stress-strain curve started to change slope significantly before that level of strain. In such cases, the stress at the point of changing the slope was recorded as the max stress. It is assumed that a significant change in slope indicates a significant crack opening.

#### **4. Results and Analysis**

A total of fifty-one slabs were tested; eight of them failed in shear and, therefore, were excluded from the results. Fig 4 shows the stress and load at failure for samples exposed to all exposures and different salts. The results will be referred to when analyzing the results of each exposure in the coming paragraphs.



#### **4.1. Control Samples**

Samples tested without salts under FT and FTWD showed failure before loading. Cracks in the middle of the slabs - under the joints - were noticed at the end of the 50 cycles and prior to loading, as shown in Fig 5. It is believed that the cracks are due to the pressure resulting from ice formation in the joints themselves rather than ice formation within the pores of the concrete. Knowing that pressure produced due to freezing of salt solution is lower than that of ice formation from pure water (Valenza et al. 2005), it was thought that slabs tested under freezing/thawing in the presence of salts are unlikely to fail in the same way. This assumption was confirmed when analyzing the results of exposures with salts. Under salt exposures, the tested samples showed a considerable load before failure, while the load in the case of the cracked control samples was negligible. Moreover, the results under salt exposures showed that cycles of FTWD cause more damage than FT alone, even though FTWD cycles have only 25 cycles of freezing/thawing compared to 50 cycles in the case of FT. This observation confirms that pressure produced from ice formation in the joints did not have a role in the damage when tested with salt solutions; otherwise, samples under FT would have shown lower strength. The control sample tested under wetting/during did not fail the same way and was used as the control or baseline sample for comparison with salt exposures.

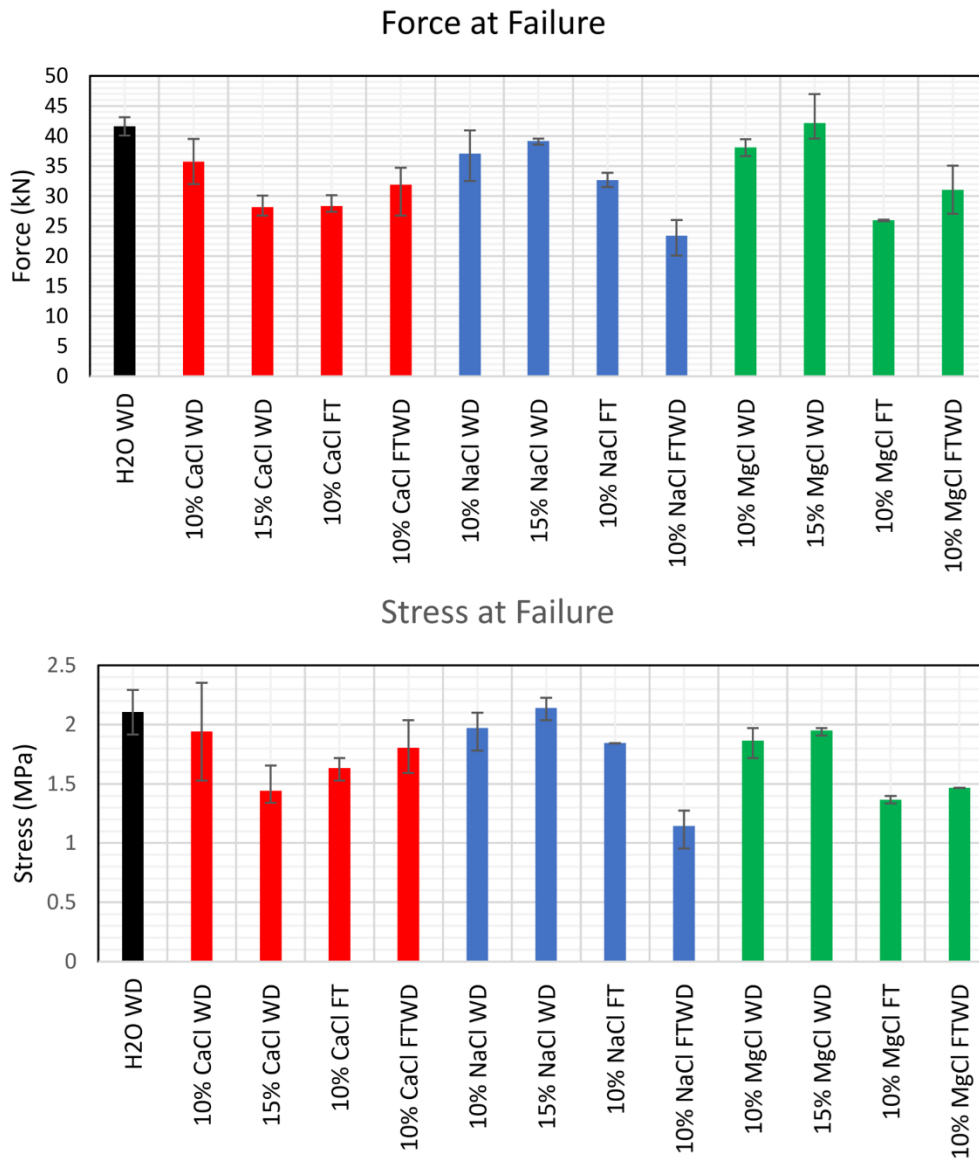


**Fig. 4.** Load at failure and stress for all exposures: (i) black: control using water in WD, (ii) red: calcium chloride, (iii) blue, sodium chloride, and (iv) green: magnesium chloride. Error bar represents min/max.



**Fig. 5.** Typical cracks developed in control samples under FT and FTW at the end of the 50 cycles

#### **4.2. Testing with Calcium Chloride**

The stress-strain curves for slabs exposed to calcium chloride are shown in Fig. 6. The weaker slabs - those that suffered more deterioration - tend to have stress-strain curves of lower slope, which becomes even lower when approaching the maximum stress. Samples tested under FT or FTWD showed stress-strain curves of slope lower than that of the control. It can be seen that the 15%  $\text{CaCl}_2$  WD exposure produced a significantly weaker stress-strain curve with a lower slope compared to any other exposures while also having the lowest load at failure. The damaging effect of high salt concentrations is manifested when comparing 10% to 15%  $\text{CaCl}_2$  under WD, where the slope of the curve and the ultimate stress are lower in the case of 15%. On the other hand, the control sample,  $\text{H}_2\text{O}$  under wetting and drying exposure, is one of the highest on the stress axis with the highest load at failure. In Fig. 4, the loads and stresses at failure for each exposure are plotted in a bar chart for ease of comparison.

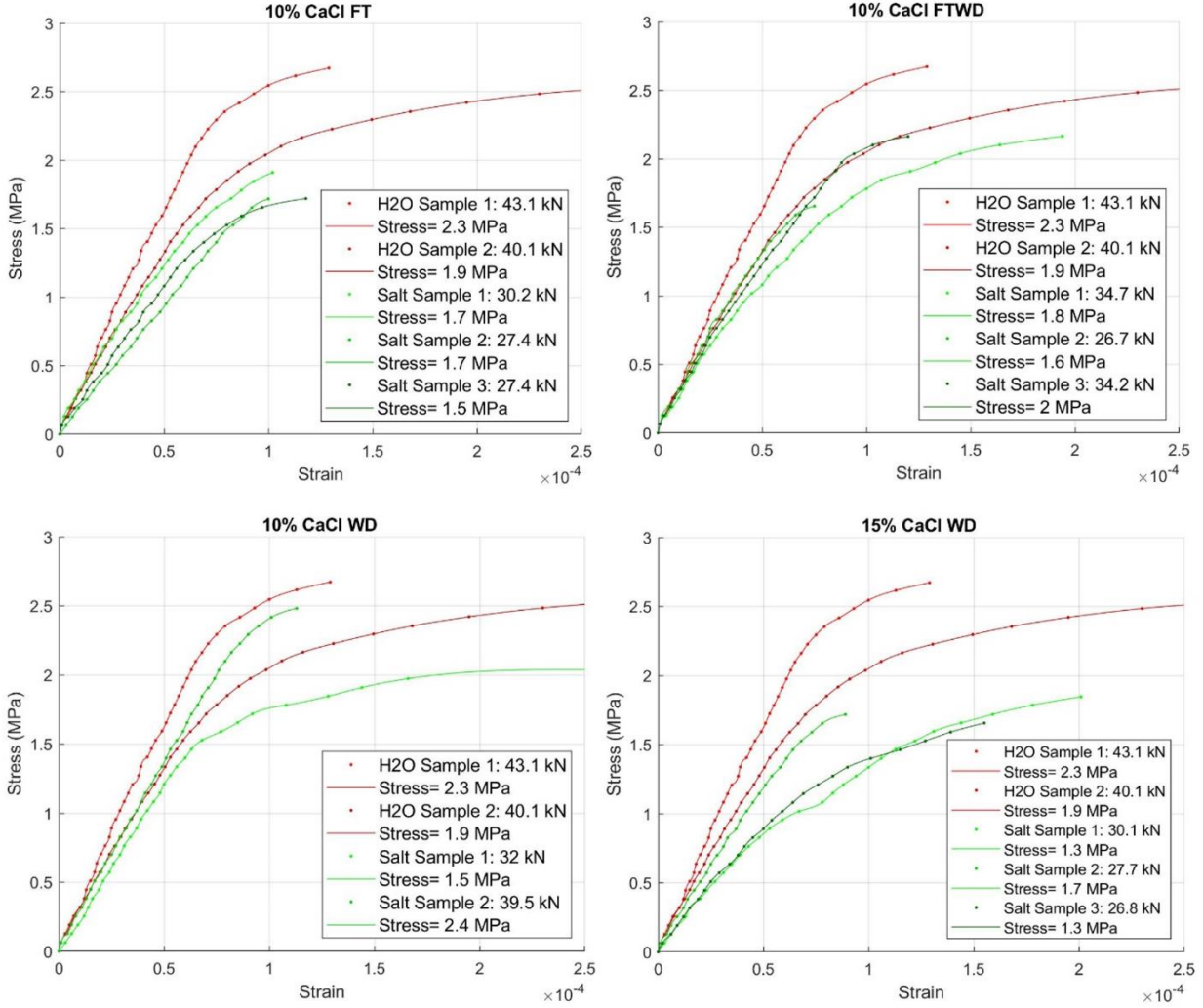


**Fig. 6.** Stress-Strain curves for slabs exposed to calcium chloride under different exposures. The reported force in the legend is the maximum load at failure, and reported stress is measured at 100  $\mu$ -strain or when the slope of the stress-strain curve changes significantly. H<sub>2</sub>O sample is the control sample tested under WD.

As presented in Fig. 4, both the force and stress portray similar relative performance for each exposure. As expected, the water control sample - under WD exposure - showed the highest strength. It is interesting to note the difference between the samples under wetting/drying at 10% and 15% concentrations. The strength of the 10% concentration sample under WD decreased slightly from the control sample while upholding relatively higher strength than the rest of the exposures, although this sample suffered significant visible damage, as will be shown later. The

15% concentration sample - on the other hand - suffered a noticeable loss in strength as well as visual damage. Using 10% concentrations, FT or FTWD showed lower strength than the control samples with no significant difference between both exposures. The damage due to freezing and thawing under the presence of salts is likely due to the reduced efficiency of the entrained air system under the presence of salts, as will be discussed in the upcoming subsections.

In addition to evaluating force and stress-strain curves, samples were inspected for visual damage. As observed from Fig. 7 and Fig. 8, both samples tested in WD showed higher spalling and cracking levels compared to other exposures, with the sample tested with 15% concentration showing greater damage than the one tested with 10% concentration. The other two samples, the 10%  $\text{CaCl}_2$  FTWD and 10%  $\text{CaCl}_2$  FT, showed no visual damage. Therefore, it can be concluded that the wetting and drying exposure leads to more damage than freezing/thawing, likely due to the production of calcium oxychloride evident by the cracking visible on the slabs. According to Qiao et al. (2018c) and Wang et al. (2019), higher calcium chloride concentrations and greater exposure duration lead to higher levels of calcium oxychloride production. As stated earlier, higher levels of damage were produced in the 15% WD samples, followed by the 10% WD samples, while no cracking was present in the 10% FT or FTWD. Under FTWD exposure, the sample was only exposed to 25 cycles of wet-dry; therefore, it is apparent that the number of cycles is not enough to produce sufficient levels of chemical damage or expansion that lead to surface cracking during the test duration. Consequently, it can be concluded that the plausible formation of calcium oxychloride results in critical damage at high concentrations such as 15% or higher, while the 10% concentration appears to be slower in promoting damage during 50 cycles of wetting and drying. Likely, for the oxychloride expansion inside the pores of the concrete to inflict visible damage and reflect a significant reduction in flexural strength, high quantities of the compound (oxychloride)

need to be present, which requires high concentration and long-enough exposure. This aligns with the work of Qiao et al. (2018c), in which a significant drop in flexural strength occurred only once the calcium chloride saturation surpassed above 20% concentration levels, which was sufficient given the large surface area exposure of the tested disc samples.

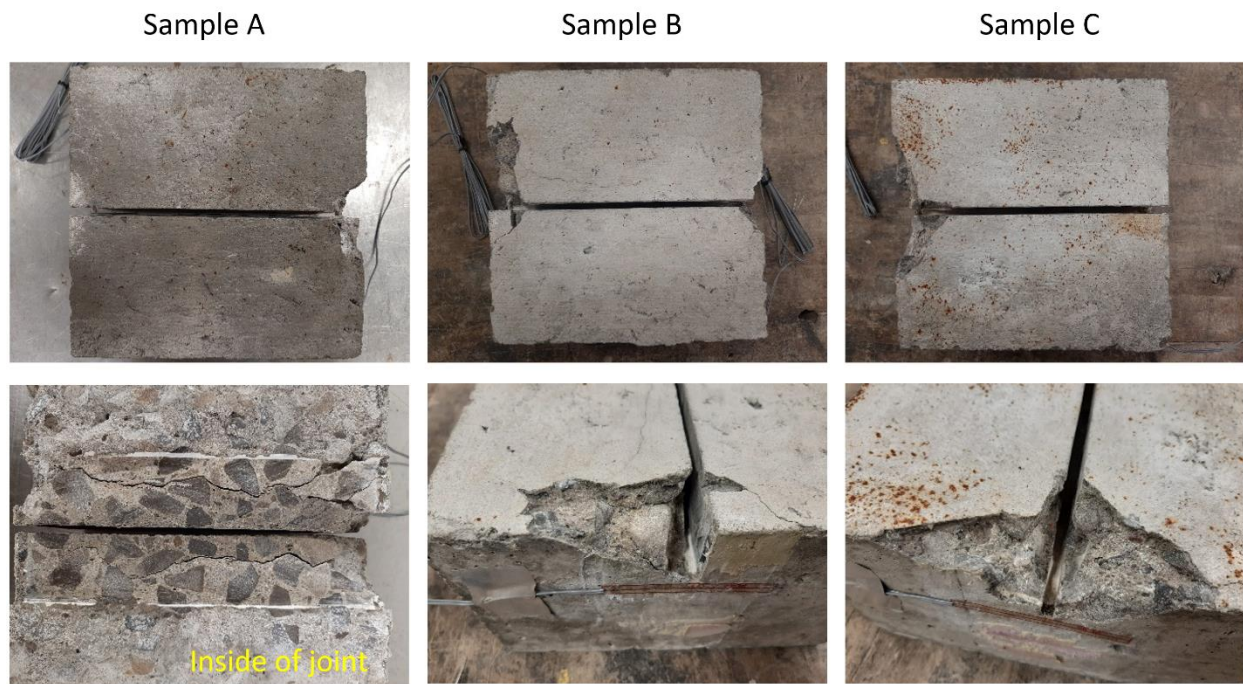


**Fig. 7.** Visual damage for 15%  $\text{CaCl}_2$  under WD





**Fig. 8.** Visual damage for 10%  $\text{CaCl}_2$  under WD

It is evident that in the case of calcium chloride under WD cycles, visual damage occurs before reduced strength, as reflected from the case of 10% concentration. The reason is that a reduced strength requires the salt to penetrate deeper below the joints to affect the bending test. Hence, both strength loss and visual damage assessment are required to evaluate the results.

#### **4.3. Testing using Sodium Chloride**

The results of testing with sodium chloride are shown in Figures 4, 9, and 10 covering the recorded maximum load and stress, the stress-strain curves, and the visual damage, respectively. Figure 9 shows that - unlike the case with calcium chloride - exposure WD did not show a change in the slope of stress-strain curves compared to that of the control. Also, exposure WD did not show a reduction in strength, as in Figure 4. By looking at Fig. 10, the salt appears to have precipitated around the joint with no visible damage under any of the exposures. The findings under WD cycles

correspond with the study of Betancourt et al. (2009) that showed the absence of appreciable deterioration due to chemical attack under exposure to sodium chloride.

The 10% FT sample shows a slight reduction in flexural strength relative to the control sample. This is likely due to the reduced efficacy of the air void system under cycles of freezing/thawing in the presence of salts. The reduced efficacy of the air-void system is better manifested under the 10% FTWD, where the WD cycles promote more salt crystallization. The formation of NaCl crystals and Friedel's salt during wetting and drying combined with cycles of freezing and thawing resulted in considerable damage. This aligns with the belief that the air voids were filled with NaCl crystals and/or Friedel's salt (Ghazi and Bassuoni 2019) which hinders the entrained air system's functionality during freeze-thaw cycles. Similar conclusions have been derived in the study of Farnam et al. (2015b), where samples that underwent freezing and thawing at high concentrations of salts (but still enough to allow for freezing) caused more damage than lower concentrations, likely due to higher crystallization.



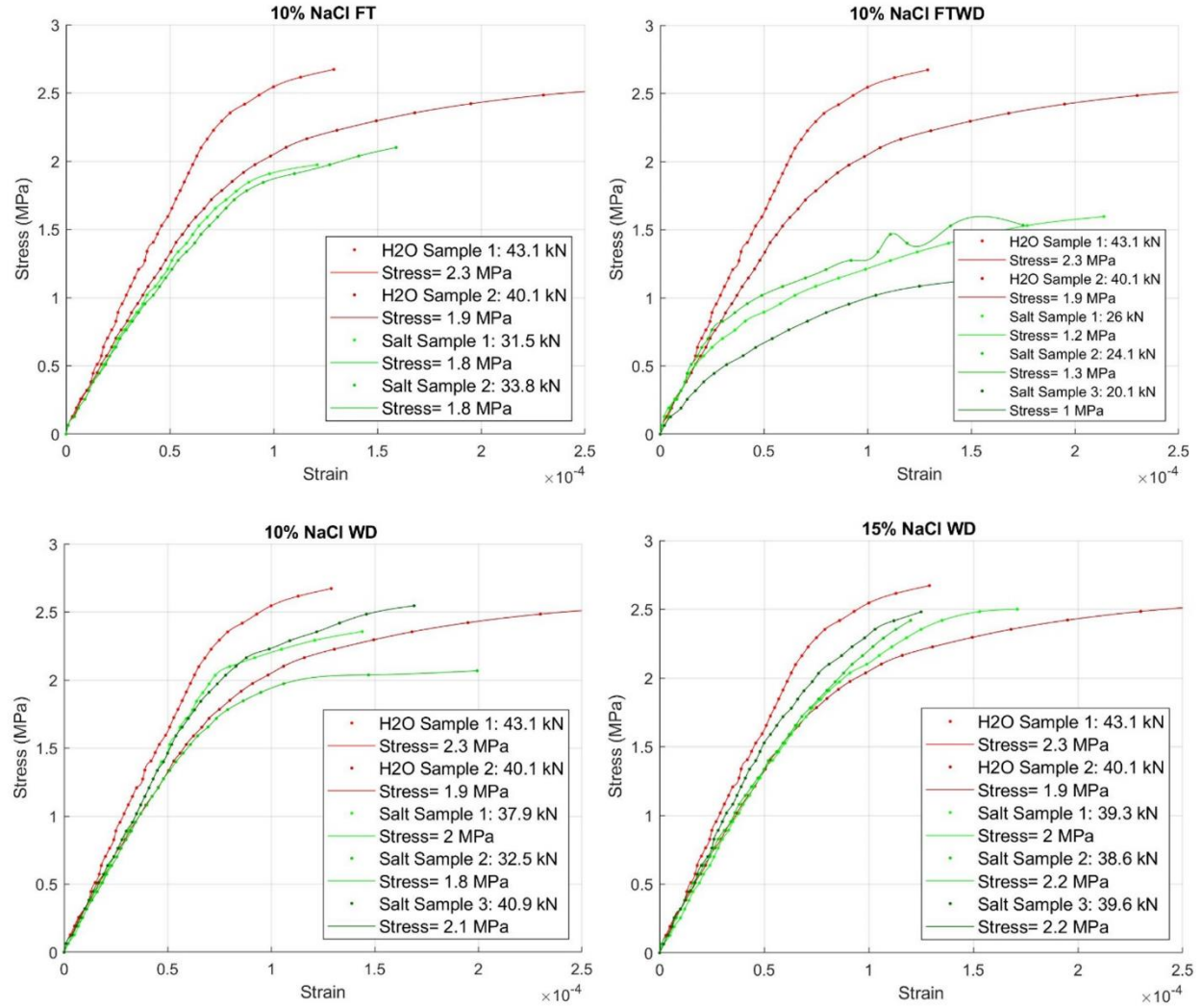


**Fig. 9.** Stress-Strain curves for slabs exposed to sodium chloride under different exposures. The reported force in the legend is the maximum load at failure, and reported stress is measured at 100  $\mu$ -strain or when the slope of the stress-strain curve changes significantly. H<sub>2</sub>O sample is the control sample tested under WD.

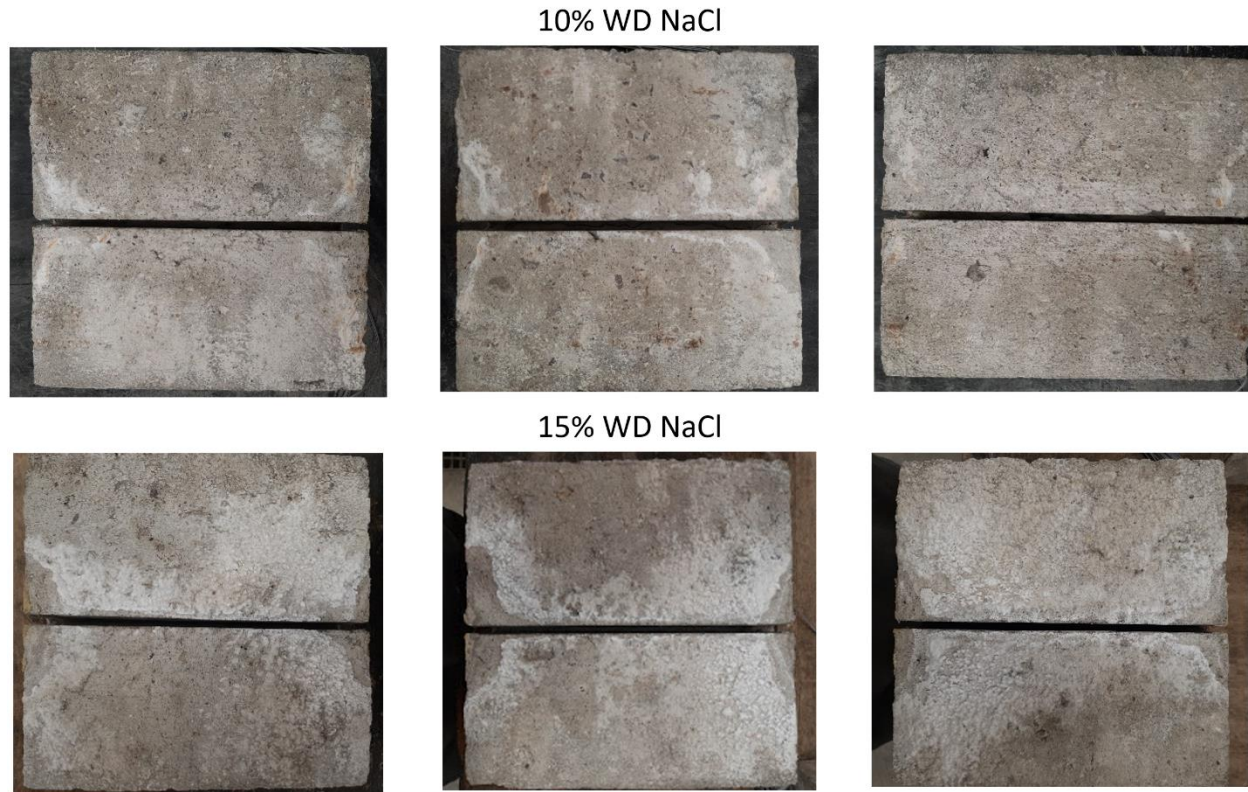


**Fig. 10.** Slab condition of 10% and 15% NaCl after 50 cycles of wetting-drying

#### 4.4. Testing using Magnesium Chloride

Fig. 11 displays the stress-strain curves of all the samples under different exposure conditions. Samples tested with 10% and 15% concentrations under cycles of wetting and drying did not show much strength loss compared to control samples; this is also shown in Fig. 4. Magnesium chloride's chemical reaction with cement paste results in de-calcification of the C-S-H and produces calcium chloride, which then forms the expansive calcium oxychloride (Farnam et al. 2015c, Xie et al. 2019). Therefore, it should be expected that the chemical reaction between high concentrations of salt would cause significant deterioration. However, the reaction also produces magnesium hydroxide or brucite. This is known to cause blockage of pores near the surface where the concrete is exposed to the salt (Farnam et al. 2015c).

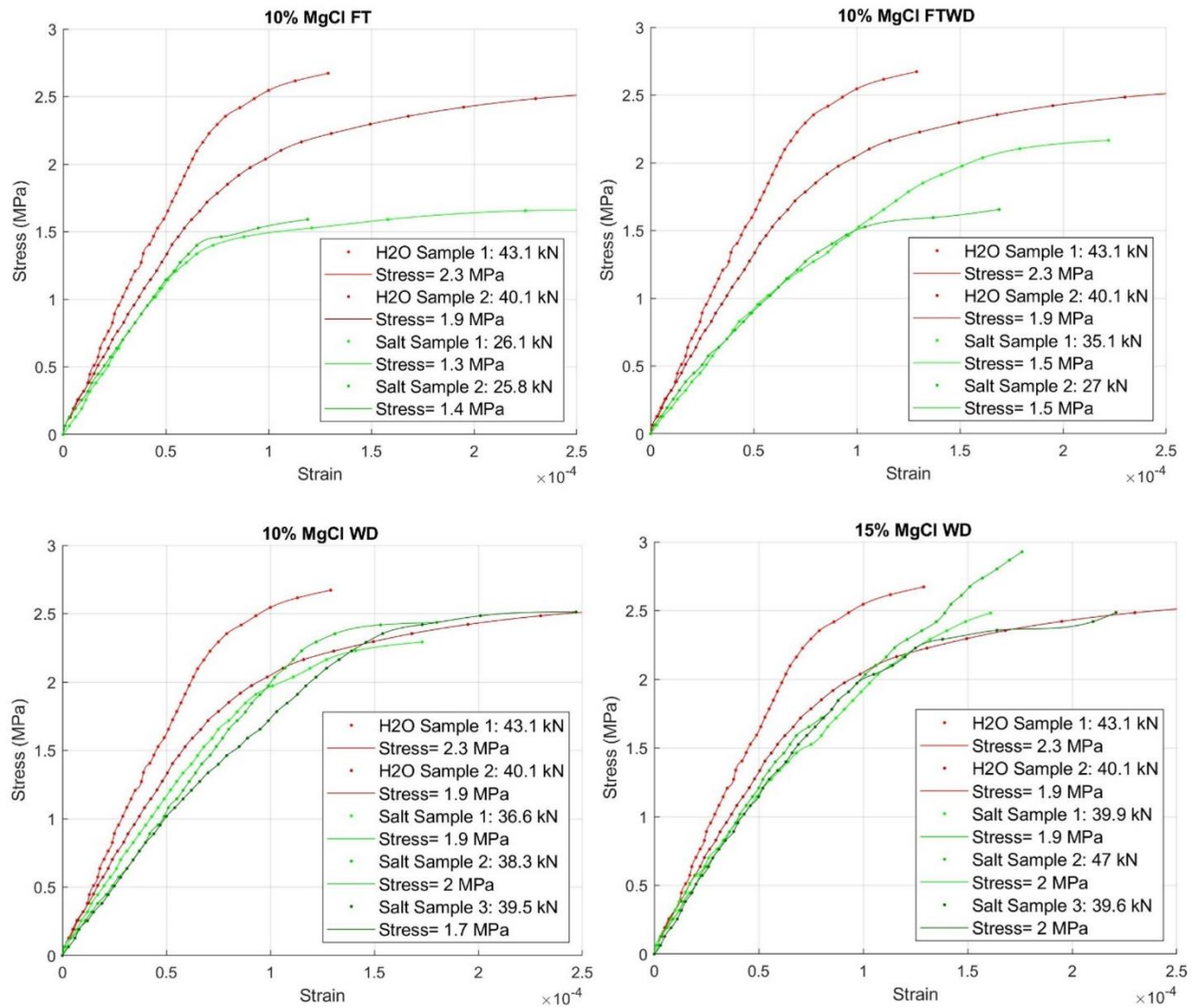


**Fig. 11.** Stress-Strain curves for slabs exposed to magnesium chloride under different exposures. Reported force is the maximum load at failure, and reported stresses in the legend are measured at 100  $\mu$ -strain or when the slope of the stress-strain curve changes significantly. H<sub>2</sub>O sample is the control sample tested under WD.

Fig. 12 shows the condition of the slabs after the wetting and drying cycles were completed for both 10% and 15% concentrations. Neither slabs exhibited any degree of cracking, which suggests the lack of considerable calcium oxychloride formation, unlike the case with the slabs exposed to calcium chloride. Studies by Peterson et al. (2013) also displayed similar observations, where the



specimens soaked in high  $\text{CaCl}_2$  concentration showed significantly more cracking and spalling than those soaked in high  $\text{MgCl}_2$  concentration. Therefore, it can be deduced that high concentrations of magnesium chloride lead to a high level of brucite, suppressing the salt's ingress into the slab and preventing significant deterioration from occurring. Alternatively, calcium oxychloride formation might be easier or faster under exposure to calcium chloride rather than magnesium chloride.

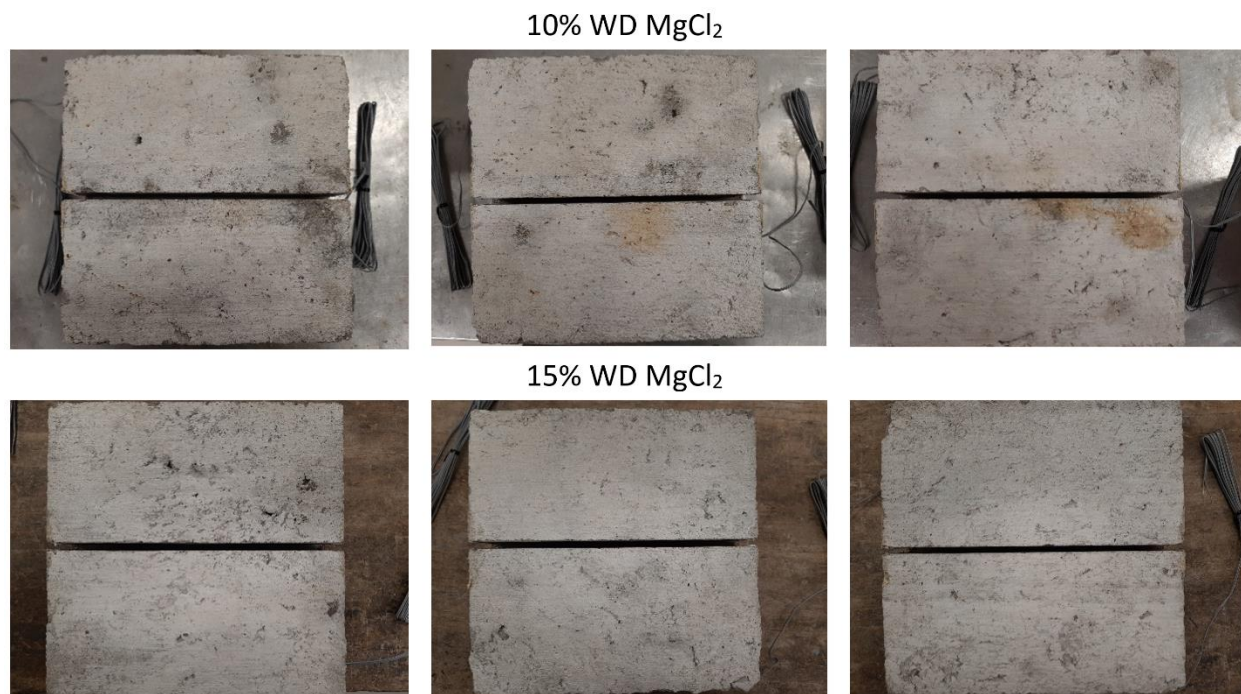


**Fig. 12.** Slab condition of 10% and 15%  $\text{MgCl}_2$  after 50 cycles of wetting-drying

According to Sutter et al. (2006), petrographic evidence revealed the formation of calcium oxychloride in samples soaked in a high concentration of magnesium chloride; however, the exposure duration was long. As such, the wetting and drying cycles did not deviate substantially from the control sample, with the 10% concentration being slightly weaker. This might not represent the actual field conditions as extended time might be needed to promote damaging chemical reactions such as decomposition of CSH. Studies by Qiao et al. (2018d) indicate that

longer exposure duration leads to more significant strength loss. Unlike WD exposure, the 10% FTWD and 10% FT slabs showed a noticeable reduction in strength relative to the control samples. It can be seen in Fig. 11 that the slope of the stress-strain curve of the 10% FT sample is similar to that of the control, with failure occurring at lower stress. On the other hand, the 10% FTWD has a noticeably lower and more non-linear slope suggesting more weakening. The results suggest that under repeated FTWD cycles, the solution found its way to the entrained-air system, causing some precipitation and reduced resistance to cycles of freezing/thawing.

## **5. Discussion**

The main objective of this study is to put the basis for a test procedure to evaluate the durability of control joints in concrete pavements. Slab samples with joints constructed to mimic construction practice in the industry were tested. Different salts and exposure conditions were tried in an attempt to establish the test conditions and salt/type concentrations that produce visible and/or measurable damage that reflect deterioration under field exposures as reported in the literature (Taylor et al. 2016, Ghazi et al. 2018, Chan et al. 2020). Standard test methods or modified versions thereof could be used to evaluate the resistance of different concrete mixes to different salt under a variety of exposures. However, the test investigated here is intended to evaluate different joint designs (width and geometry) and construction practices such as curing and forming joints (pre-molded versus saw cut and method of saw cutting). This paper focused on establishing the conditions and salt type/concentrations that lead to deterioration in a relatively short time.

As presented in the results, different salts produce different levels of damage under different exposures. Calcium chloride is known to form oxychloride that expands within the pores of the concrete. The reaction is optimum at 5 °C, where the calcium oxychloride is stable without the

need for freezing. The above reasons are why the 15% WD exposure investigated here was best at capturing the deterioration caused by this deicer.

Sodium chloride reacts with the cement paste and forms Friedel's salt and Kuzel's salt. It was shown that deterioration is maximized when large quantities of salt are present when the slab undergoes freezing. The salt resides in the concrete air-entraining system inhibiting its use as expansion chambers for ice formation. As a result, the 10% FTWD exposure was most effective at representing the damage. Perhaps a higher concentration might have produced more damage.

Finally, the de-calcification of concrete when exposed to magnesium chloride was not produced in this study due to: (i) the production and precipitation of magnesium hydroxide or brucite on the concrete surface reducing salt penetration, and/or (ii) the fifty cycles of wetting and drying was not enough to accelerate the chemical reactions due to the slow ingress of the salt into the concrete.

It should be noted that the purpose of introducing the wetting and drying cycles is to sustain chemical attacks and promote the crystallization of salts within the air voids and the pores of the concrete to accelerate the damage. However, under cycles of freezing and thawing alone, salt crystals can also fill air voids, reducing the entrained air efficacy in resisting freezing/thawing cycles. Fig. 13 shows a Backscattered Electron Image (BSE) of samples investigated in an earlier study by the same research team at Ryerson (Babic 2019). The samples were exposed to FT cycles using 3% NaCl, and 3% and 10% CaCl<sub>2</sub>. The images show partially-filled air voids with cracked pastes in samples tested under 3% CaCl<sub>2</sub> (Fig. 13a) and 3% NaCl (Fig. 13b). The level of air-voids filling is greater when a higher concentration of salt was used, as shown in Fig. 13c for samples tested under 10% CaCl<sub>2</sub>. It is believed that the reduced strength obtained under FT or FTWD cycles - is attributed to the same observation shown in Figure 13.

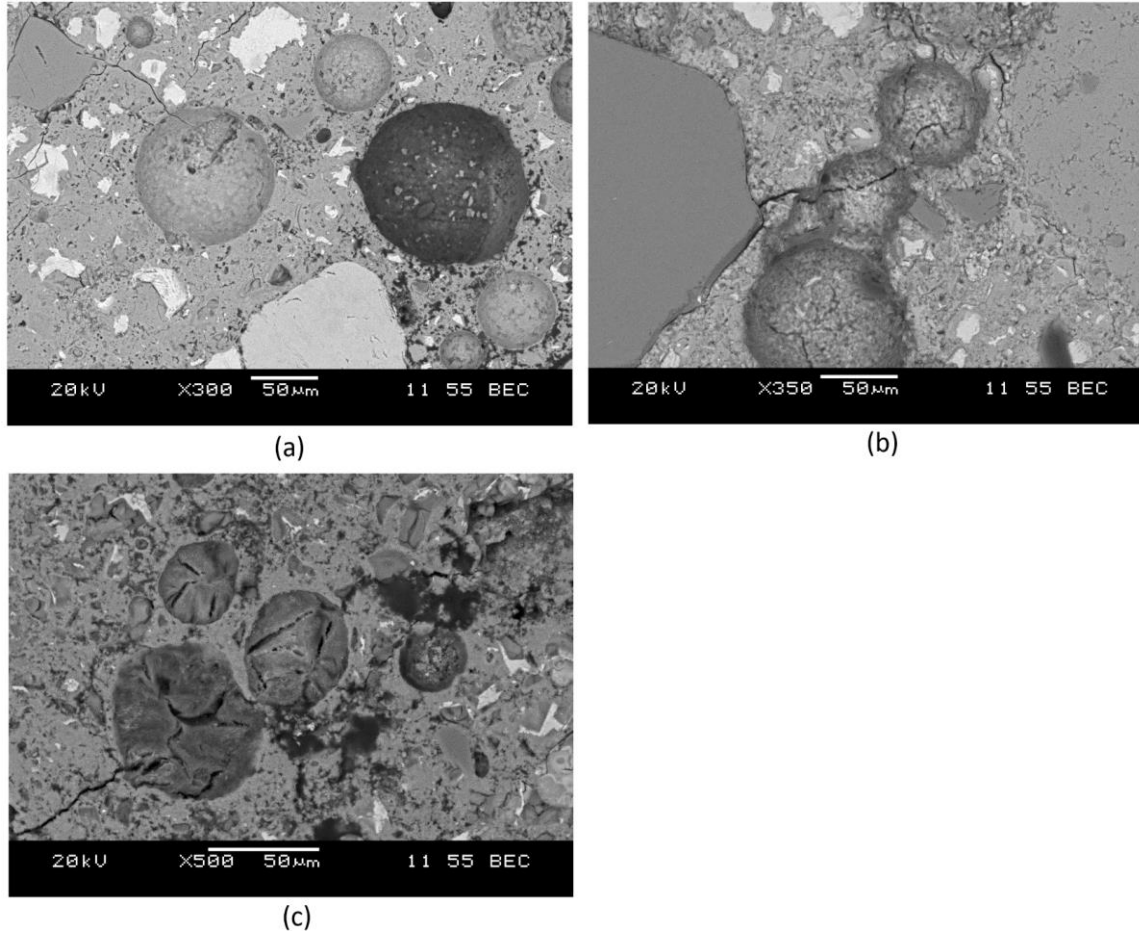


**Fig. 13.** BSE Images taking by Scanning Electron Microscope showing entrained air voids for samples tested under 50 cycles of FT using: (a) 3% CaCl<sub>2</sub>, (b) 3% NaCl, and (c) 10% CaCl<sub>2</sub>

The visual damage observed here was mainly in the form of spalling and cracking, similar to what was observed under field exposure (Chan et al. 2020). Based on the tested samples, a visual index of more than two steps (damaged or undamaged) could not be developed here. Also, a more detailed index covering crack width and density could not be established as it requires more testing. Based on the results, samples could be classified as damaged or no damage, as shown in Fig. 14.



**Fig. 14.** Visual Damage Classification

Based on the obtained results, the following conditions and evaluation methods were found promising in evaluating the durability of joints: (i) 10% NaCl FTWD and (ii) 15% CaCl<sub>2</sub> WD. The first exposure tests the physical damage resulting from freezing/thawing cycles and crystallization of salt within the concrete pores and entrained air. The second exposure - 15% CaCl<sub>2</sub> WD - focuses on the stability of the mixtures in terms of a chemical attack. The evaluation method should include



both: visual damage and load/stress at failure as described here. It is recommended to test joints using both exposures as each one evaluates a different form of attack. For testing the slabs in bending, it was found here that the load at failure and the stress under the joint produce the same conclusions or outputs. Accordingly, the load at failure alone can be used for evaluating the strength reduction after testing. For visual evaluation, it is recommended that a picture of the slab be taken before and after the test to confirm the damage induced during the test. In addition to evaluating different joint configurations, the test can be used to evaluate the aggressiveness of different salts. In addition, the test can be extended to compare concrete mixes.

The sample size/preparation can benefit from some modifications. For example, the damage that was observed before loading in the case of using freshwater under freezing/thawing could be eliminated in future testing. One way of addressing this is to restrain the two sides of the joints from opening up using clamps. This would simulate the field situation where the joints can not open up easily due to the size of the pavement. The dimension of the slab can be modified slightly to prevent failure under shear, which was found in limited cases here. Finally, the concrete tested here has strength and - to some extent - air content lower than that required for concrete pavements in Canada. A mix of this level of strength and air content would be used in the test to compare the efficacy of different joint designs, i.e., depth, width, geometry, and use of sealant. For comparing concrete of different strengths, the same method can be used - perhaps with an extension of the testing period. This requires further research to determine the required number of cycles.

## **6. Conclusions**

1. A lab method is introduced to assess the durability of control joints in concrete under different freezing/thawing and wetting/drying cycles.
2. High concentrations of calcium chloride (>10%) were found to cause spalling and cracking when the test sample undergoes wetting/drying cycles; the damage was visible.
3. Sodium chloride produced damage in the form of strength reduction when the slab underwent combined cycles of freezing/thawing and wetting/drying; no visible damage was observed.
4. Magnesium chloride needed a more prolonged exposure duration to induce damage
5. A test method is recommended with two exposures: sodium chloride at 10% under FTWD and calcium chloride at 15% under WD. The damage is assessed using visual evaluation and strength loss under flexural loading.

## **7. Acknowledgments**

Funding for this research was provided through the Ministry of Transportation, Ontario (MTO) Highway Infrastructure Innovation Fund and Natural Sciences and Engineering Canada (NSERC) Discovery grant. The opinions expressed in this paper are those of the authors and may not necessarily reflect the views and policies of MTO. The authors acknowledge the support of Ms. Melissa Titherington of MTO for providing data of deteriorated pavements and Mr. Conrad Babicz of Ryerson University for the Scanning Electron Microscopy images. This research was also supported by the Ryerson University Faculty of Engineering and Architectural Science Dean's Research Fund.

## **9. Contributors Statement**

Ramy Elbakari: investigation, formal analysis, writing - original draft, visualization

Medhat Shehata: supervision, writing - review and editing, project administration, funding acquisition

## **10. Competing interests: formal analysis, investigation**

The authors declare there are no competing interests.

## **11. References**

ASTM C666 / C666M-15, Standard Test Method for Resistance of Concrete to Rapid Freezing and Thawing, ASTM International, West Conshohocken, PA, 2015, [www.astm.org](http://www.astm.org)

Babicz, C. 2019. Development of a Test Method to Evaluate Durability of Pavement Joints Under Winter Conditions. Master of Applied Science Thesis, Ryerson University, Toronto, Ontario.

Bathe, K.J. 2006. *Finite element procedures*. Klaus-Jurgen Bathe. Prentice-Hall, Inc., Upper Saddle River, NJ

Betancourt, G.A.J. 2009. *Effect of De-icer and Anti-icer Chemicals on the Durability, Microstructure, and Properties of Cement-based Materials* (Doctoral dissertation University of Toronto, Toronto, Ontario).

Chan, S., Titherington, M. & Lee, S. 2020. Specification Improvement to Deliver Safe and Durable Concrete Pavement in Ontario. In *Transportation Association of Canada 2020 Conference and Exhibition-The Journey to Safer Roads*.

Chatterji, S. 1978. Mechanism of the  $\text{CaCl}_2$  attack on portland cement concrete. *Cement and Concrete Research*, 8(4), pp.461-467.

A23.2-22C, Scaling resistance of concrete surfaces exposed to deicing chemicals using mass loss, Canadian Standard Association, CSA A23.1:19/CSA A23.2:19, Toronto, Ontario, Canada.

Delatte, N.J. 2014. Concrete Pavement Design, Construction, and Performance (2nd ed.). CRC Press. <https://doi-org.ezproxy.lib.ryerson.ca/10.1201/b17043>

Farnam, Y., Dick, S., Wiese, A., Davis, J., Bentz, D. and Weiss, J. 2015a. The influence of calcium chloride deicing salt on phase changes and damage development in cementitious materials. *Cement and Concrete Composites*, 64, pp.1-15.

Farnam, Y., Todak, H., Spragg, R. and Weiss, J. 2015b. Electrical response of mortar with different degrees of saturation and deicing salt solutions during freezing and thawing. *Cement and Concrete Composites*, 59, pp.49-59.

Farnam, Y., Wiese, A., Bentz, D., Davis, J. and Weiss, J. 2015c. Damage development in cementitious materials exposed to magnesium chloride deicing salt. *Construction and Building Materials*, 93, pp.384-392.

Federal Highway Administration, 2019. Report No. T 5040.30: Concrete Pavement Joints.

Available on line: <https://www.fhwa.dot.gov/pavement/ta504030.pdf>

Ghazy, A., Bassuoni, M. T., & Islam, A. K. M. R. 2018. Assessment of Joints in Concrete Pavements Exposed to Different Winter Conditions. *Journal of performance of constructed facilities*, 32(2): 04017135. DOI: 10.1061/(ASCE)CF.1943-5509.0001131

Ghazy, A., and Bassuoni, M. 2019. Response of concrete to cyclic environments and chloride-based salts. *Journal: Magazine of concrete research*, 71(10). DOI: 10.1680/jmacr.17.00454

Heukamp, F.H., Ulm, F.J. and Germaine, J.T. 2001. Mechanical properties of calcium-leached cement pastes: triaxial stress states and the influence of the pore pressures. *Cement and Concrete Research*, 31(5), pp.767-774.

Jones, W., Farnam, Y., Imbrock, P., Spiro, J., Villani, C., Olek, J. and Weiss, W.J. 2013. An overview of joint deterioration in concrete pavement: Mechanisms, solution properties, and sealers. Purdue University, West Lafayette, Indiana.

Jones, C., Ramanathan, S., P., and Hale, W.M. 2020. Calcium oxychloride: A critical review of the literature surrounding the formation, deterioration, testing procedures, and recommended mitigation techniques. *Cement and Concrete Composites*, 113, 103663.

<https://doi.org/10.1016/j.cemconcomp.2020.103663>

OPSS 2021, Ontario Provisional Standards Specification, Material Requirements, Vol. 8, Division 25 – Chemicals

Peterson, K., Julio-Betancourt, G., Sutter, L., Hooton, R.D. and Johnston, D. 2013. Observations of chloride ingress and calcium oxychloride formation in laboratory concrete and mortar at 5 C. *Cement and Concrete Research*, 45, pp.79-90.

- Qiao, C., Ni, W., Wang, Q. and Weiss, J. 2018a. Chloride diffusion and wicking in concrete exposed to NaCl and MgCl<sub>2</sub> solutions. *Journal of Materials in Civil Engineering*, 30(3), p.04018015.
- Qiao, C., Suraneni, P. and Weiss, J. 2018b. Damage in cement pastes exposed to NaCl solutions. *Construction and Building Materials*, 171, pp.120-127.
- Qiao, C., Suraneni, P. and Weiss, J. 2018c. Flexural strength reduction of cement pastes exposed to CaCl<sub>2</sub> solutions. *Cement and Concrete Composites*, 86, pp.297-305.
- Qiao, C., Suraneni, P., Chang, M.T. and Weiss, J. 2018d. Damage in cement pastes exposed to MgCl<sub>2</sub> solutions. *Materials and Structures*, 51(3), p.74.
- Suraneni, P., Azad, V.J., Isgor, O.B. and Weiss, W.J. 2016. Deicing salts and durability of concrete pavements and joints. *Concr. Int*, 38(4), pp.48-54.
- Sutter, L., Peterson, K., Touton, S., Van Dam, T. and Johnston, D. 2006. Petrographic evidence of calcium oxychloride formation in mortars exposed to magnesium chloride solution. *Cement and Concrete Research*, 36(8), pp.1533-1541.
- Taylor, P., Sutter, L. and Weiss, J. 2012. Investigation of deterioration in joints in concrete pavements. Report No. InTrans Project 09-361. Joint Transportation Research Program, Iowa State University and Federal Highway Administration, Washington, DC.
- Taylor, P., Zhang, J., & Wang, X. 2016. Conclusions from the Investigation of Deterioration of Joints in Concrete Pavements. Iowa State University Institute for Transportation: National Concrete Pavement Technology Center.

Thaulow, N. and Sahu, S. 2004. Mechanism of concrete deterioration due to salt crystallization. *Materials Characterization*, 53(2-4), pp.123-127.

Valenza, J.J. and Scherer, G.W. 2005. Mechanisms of salt scaling. *Materials and Structures*, 38(4), pp.479-488.

Wang, K., Nelsen, D.E. and Nixon, W.A. 2006. Damaging effects of deicing chemicals on concrete materials. *Cement and concrete composites*, 28(2), pp.173-188.

Wang, X., Zhang, J., Wang, X., Taylor, P., Wang, K., and Xinjian, S. 2018. Exploration of Mechanisms of Joint Deterioration in Concrete Pavements regarding Interfacial Transition Zone. Article ID 3295954, 9 pages, <https://doi.org/10.1155/2018/3295954>

Wang, X., Sadati, S., Taylor, P., Li, C., Wang, X., and Sha, A. 2019. Material characterization to assess effectiveness of surface treatment to prevent joint deterioration from oxychloride formation mechanism. *Cement and Concrete Composites*, 103394. <https://doi.org/10.1016/j.cemconcomp.2019.103394>

Xie, N., Dang, Y., and Shid, X. 2019. New insights into how  $MgCl_2$  deteriorates Portland cement concrete. *Cement and Concrete Research*, 120, pp 244-255

Zhang, J. , Taylor, P., and Caijun. S. 2015. Investigation of Approaches for Improving Interfacial Transition Zone-Related Freezing-and-Thawing Resistance in Concrete Pavement. *ACI Materials Journal*; 112(5): 613-617. DOI:0002168598; 10.14359/51687902

## List of Tables

Table 1: Test matrix and labels of cycles.

## List of Figures

**Fig. 1.** Moulds with railing to enable accurate saw cutting of the joints after hardening.

**Fig 2.** A schematic of a test slab after being enclosed on both ends of the joint and filled with the solution

**Fig.3.** a) Three-point loading of slabs until failure b) Slab dimensions and loading condition

**Fig. 4.** Load at failure and stress for all exposures: (i) black: control using water in WD, (ii) red: calcium chloride, (iii) blue, sodium chloride, and (iv) green: magnesium chloride. Error bar represents min/max.

**Fig. 5.** Typical cracks developed on FT and FTW control samples at the end of the 50 cycles

**Fig. 6.** Stress-Strain curves for slabs exposed to calcium chloride under different exposures. The reported force in the legend is the maximum load at failure, and reported stress is measured at 100  $\mu$ -strain or when the slope of the stress-strain curve changes significantly. H<sub>2</sub>O sample is the control sample. H<sub>2</sub>O sample is the control sample tested under WD.

**Fig. 7.** Visual damage for 15% WD CaCl<sub>2</sub>

**Fig. 8.** Visual damage for 10% WD CaCl<sub>2</sub>

**Fig. 9.** Stress-Strain curves for slabs exposed to sodium chloride under different exposures. The reported force in the legend is the maximum load at failure, and reported stress is measured at 100  $\mu$ -strain or when the slope of the stress-strain curve changes significantly. H<sub>2</sub>O sample is the control sample. H<sub>2</sub>O sample is the control sample tested under WD.

**Fig. 10.** Slab condition of 10% and 15% NaCl after 50 cycles of wetting-drying



**Fig. 11.** Stress-Strain curves for slabs exposed to magnesium chloride under different exposures. Reported force is the maximum load at failure, and reported stresses in the legend are measured at 100  $\mu$ -strain or when the slope of the stress-strain curve changes significantly. H<sub>2</sub>O sample is the control sample tested under WD.

**Fig. 12.** Slab condition of 10% and 15% MgCl<sub>2</sub> after 50 cycles of wetting-drying

**Fig. 13.** BSE Images taking by Scanning Electron Microscope showing entrained air voids for samples tested under 50 cycles of FT using: (a) 3% CaCl<sub>2</sub>, (b) 3% NaCl, and (c) 10% CaCl<sub>2</sub>

**Fig. 14.** Visual Damage Classification